

RESEARCH ARTICLE

Low Emissions and Delay Optimization for an Isolated Signalized Intersection Based on Vehicular Trajectories

Ciyun Lin^{1,2}*, Bowen Gong^{1,2}*, Xin Qu²*

1 State Key Laboratory of Automobile Dynamic Simulation, Jilin University, Changchun, 130022, China, **2** College of Transportation, Jilin University, Changchun, 130022, China

* These authors contributed equally to this work.

* linciyun@jlu.edu.cn (LCY); gongbowen@jlu.edu.cn (GBW); quxin14@mails.jlu.edu.cn (QX)



OPEN ACCESS

Citation: Lin C, Gong B, Qu X (2015) Low Emissions and Delay Optimization for an Isolated Signalized Intersection Based on Vehicular Trajectories. PLoS ONE 10(12): e0146018. doi:10.1371/journal.pone.0146018

Editor: Tiejiao Tang, Beihang University, CHINA

Received: July 7, 2015

Accepted: December 12, 2015

Published: December 31, 2015

Copyright: © 2015 Lin et al. This is an open access article distributed under the terms of the [Creative Commons Attribution License](https://creativecommons.org/licenses/by/4.0/), which permits unrestricted use, distribution, and reproduction in any medium, provided the original author and source are credited.

Data Availability Statement: All relevant data are within the paper and its Supporting Information files.

Funding: This work was supported by the National Science Foundation of China (Grant No. 51408257 and No. 51308248), the Chinese National High Technology Research and Development Program (Grant No. 2014BAG03B03), the Specialized Research Fund for the Doctoral Program of Higher Education of China (Grant No. 20120061120046), the National Science Foundation for Post-doctoral Scientists of China (Grant No. 2013T60331 and No.2012T50300), and the Youth Scientific Research Fund of Jilin (Grant No. 20140520134JH). The funders had no role in study design, data collection

Abstract

A traditional traffic signal control system is established based on vehicular delay, queue length, saturation and other indicators. However, due to the increasing severity of urban environmental pollution issues and the development of a resource-saving and environmentally friendly social philosophy, the development of low-carbon and energy-efficient urban transport is required. This paper first defines vehicular trajectories and the calculation of vehicular emissions based on VSP. Next, a regression analysis method is used to quantify the relationship between vehicular emissions and delay, and a traffic signal control model is established to reduce emissions and delay using the enumeration method combined with saturation constraints. Finally, one typical intersection of Changchun is selected to verify the model proposed in this paper; its performance efficiency is also compared using simulations in VISSIM. The results of this study show that the proposed model can significantly reduce vehicle delay and traffic emissions simultaneously.

Introduction

Road-based traffic emissions produce a large amount of suspended particulate matter in the air of urban cities. Traffic emissions have been shown to be the primary source of fog and haze in cities; these pollutants can cause significant problems, including reduced traffic visibility and decreased immune response in the respiratory systems of humans, etc. The studies show that the traffic fuel consumption has become an importation part of petroleum consumption and its emissions have turned a major source of air pollution[1–3]. And vehicles idling at signalized intersections often result in an increase in fuel consumption and emissions of pollutants, including CO, HC+NO_x, PM and other noxious gases. Thus researchers developed many models and traffic control methods to study the traffic emissions and to reduce vehicles idling at signalized intersection. The-state-of-the-art study for traffic emissions is to explore the influences of the vehicle's fuel consumption and exhaust emissions on the trip under different traffic conditions [4–12]. For example, researches developed car-following models to explore the impacts of the

and analysis, decision to publish, or preparation of the manuscript.

Competing Interests: The authors have declared that no competing interests exist.

vehicle’s fuel consumption and exhaust emissions[13–16]. Some researches focus on studying traffic phenomena to developed traffic flow models or new technologies to enhance traffic safety and reduce fuel consumption and traffic emissions [17–26]. Traffic signal timing and traffic states of the intersection impacts on fuel consumption and emission are studied and evaluated in the literature[27–32]. In the literature, the importance of traffic signal timing optimization is well established by several studies conducted as a result of the increase serious traffic problems. The studies developed control models or methods to explore the complex traffic phenomena and to optimize the signal timing parameters by considering temporal, spatial, or temporal-spatial costs to vehicles and travelers, such as vehicle delay, queue length, saturation, etc[33–42]. However, development of an optimization model considering both traffic performance and traffic emissions has not received the same level of attention compared with the studies of explore the relationship of fuel consumption and emission and the studies of optimal traffic signal timing to maximize the intersection’s traffic capacity while minimizing traffic delay[43–48]. Although the number of studies about optimal traffic signal timing based on emission and delay is limited for regular traffic signal control, there is an agreement on signal timing optimization play an important role in traffic flow management by reducing traffic delay and emission[49–51].

Intelligent transportation systems (ITS) have the positive effect on improving traffic operation efficiency, alleviating traffic congestion, ensuring traffic safety and reducing traffic emissions and so on. Therefore, the state and governments at all levels take serious attitude towards the development and planning strategy of ITS. The governments have put forward a series of policies to stimulate its development as to maintain the sustainability of urban traffic systems. Synchronously, China aims to build a resource-conserving and environmentally friendly society, one of the earlier and most significant works focusing on building low-carbon and energy-saving systems for transportation system. So that determining how to optimize traffic flow in an urban traffic network with low emissions and delay is the primary goal of both ITS and low-carbon and energy-saving systems.

Therefore, the goal of this study is to optimize the traffic signal control parameters to minimize both the emissions and the delay of vehicles. The parameter VSP (Vehicle Specific Power) is used to calculate the traffic emissions of a vehicle based on vehicular trajectory. In addition, the relationship between traffic emissions and delay is quantified using regression analysis. Next, an optimization model for a traffic signal control system is established, including the control variables, constraint variables (such as traffic emission and delay) and target variables.

Methods

Vehicular trajectory analysis

When a vehicle approaches a signalized intersection, the movement of the vehicle can be divided into four steps: constant speed, deceleration, queuing and acceleration. As shown in Fig 1, the red area represents the period during which the red signal is illuminated; the yellow area represents the period when the vehicle is decelerating; the light blue area represents the queuing period; and the dark blue area represents the period when the vehicle is accelerating.

The deceleration process can be described as follows:

$$S_d(t) = v_f t - 0.5a_d t^2 \tag{1}$$

$$t_d = \frac{v_f}{a_d} \tag{2}$$

$$S_d = S_d(t_d) \tag{3}$$

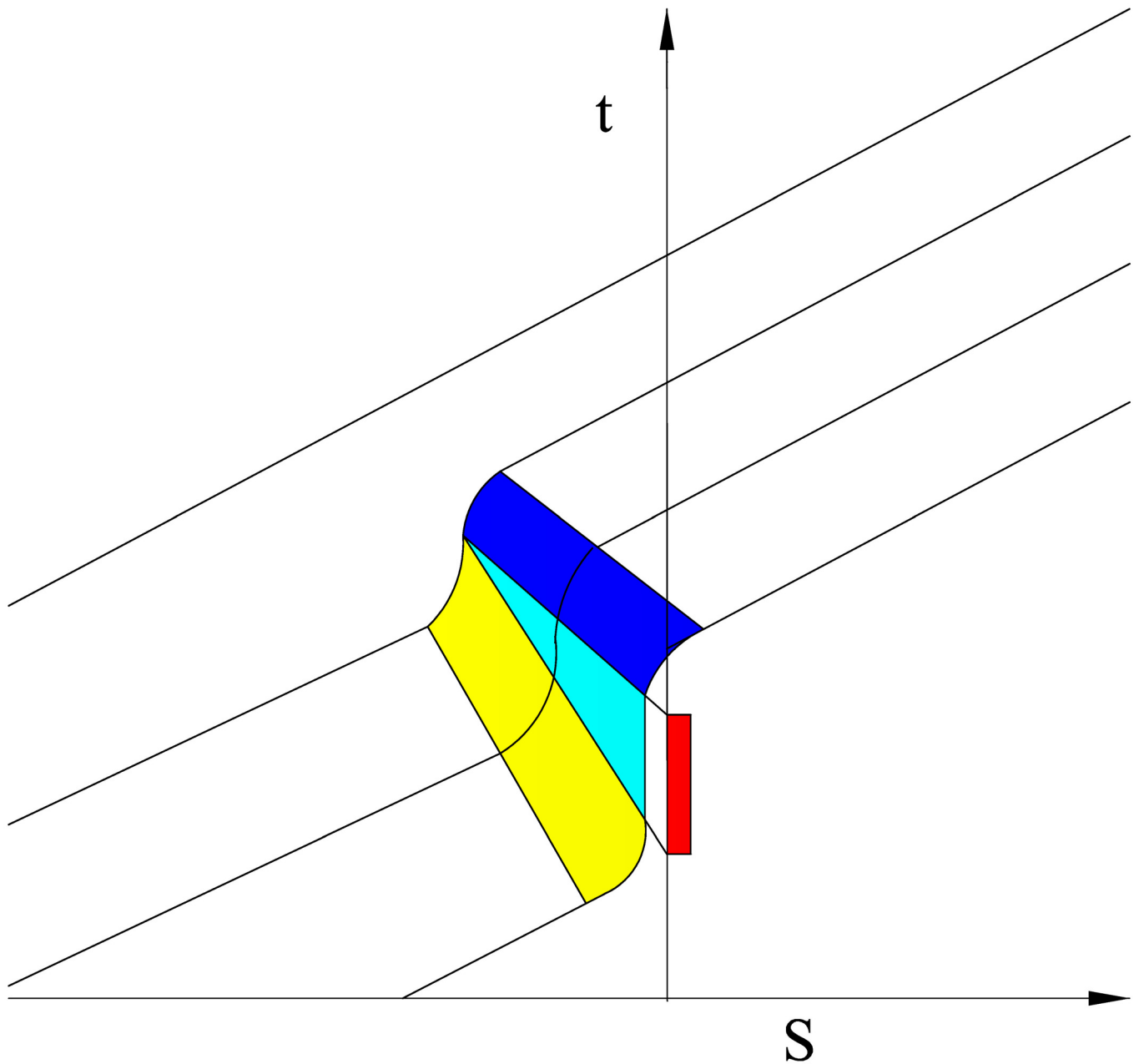


Fig 1. Vehicle trajectory diagram.

doi:10.1371/journal.pone.0146018.g001

where $S_d(t)$ is the distance function corresponding to the deceleration of the vehicle, v_f is the free-flow speed, a_d is the acceleration when the vehicle is decelerating and t_d is the duration of the vehicle's deceleration.

The acceleration process can be described by Eq 4:

$$a_a(t) = \alpha \cdot v_a(t) + b \tag{4}$$

where $a_a(t) = \frac{\partial^2 S_a(t)}{\partial t^2}$ is the acceleration of the accelerating vehicle, $v_a(t) = \frac{\partial S_a(t)}{\partial t}$ is the speed of

the accelerating vehicle at time t , $S_a(t)$ is the distance function of the accelerating vehicle, α and b are the adjustment coefficients.

The initial conditions of the vehicle's movement are given as follows. Setting $v_a(0) = 0$ and $S_a(0) = 0$, the following equations can be obtained:

$$a_a(t) = be^{\alpha t} \tag{5}$$

$$v_a(t) = \frac{b}{\alpha}(e^{\alpha t} - 1) \tag{6}$$

$$S_a(t) = \frac{b}{\alpha^2}(e^{\alpha t} - \alpha t - 1) \tag{7}$$

The duration and the distance of the accelerating vehicle can be calculated respectively as follows:

$$t_a = a_a(t) \cdot v_a^{-1}(t) \tag{8}$$

$$S_a = S_a(t_a) \tag{9}$$

From the time and distance functions as the vehicle approaches the signalized intersection, the threshold of the vehicle delay D_c can be calculated using Eqs 1 through 9, resulting in Eq 10:

$$D_c = (t_d - \frac{S_d}{v_f}) + (t_a - \frac{S_a}{v_f}) \tag{10}$$

Traffic emissions calculation

Many calculation models for vehicular emissions have been developed to date, both at home and abroad. For example, the MOBILE model and the EMFAC model are based on the driving cycle, which does not consider the engine load effect on the emissions[51–53]. The MEASURE model is based on the running state and thus does not consider the effect of the road level on the emissions[32]. The emissions model based on fuel consumption cannot describe the effects of the vehicle's movement on its emissions[42]. Based on road tests, the MOVES model was built, and a more accurate microscopic simulation was developed. However, the MOVES model is not applicable in China[50]. Therefore, a more suitable emissions model is required for China's road traffic. VSP is defined as the output power when a vehicle's engine moves one ton of mass, which best approximates the parameters of the real situation. VSP can effectively depict the real vehicular driving characteristics present on a road.

The derivation process of the VSP for vehicles can be represented by Eq 11 [54]:

$$VSP = \frac{\frac{d}{dt}(KE + PE) + p_f + 0.5\rho_a C_D A(v + v_w)^2 v}{m} \tag{11}$$

where $\frac{d}{dt}(KE + PE)$ is the power required to change the kinetic/potential energy; $p_f v$ is the power required to overcome rolling resistance; $0.5\rho_a C_D A(v + v_w)^2 v$ is the power required to overcome aerodynamic drag; KE is the kinetic energy of the vehicle; PE is the potential energy of the vehicle; p_f is the rolling resistance; m is the mass of the vehicle (kg); v is the vehicle speed (m/s); v_w is the wind speed of the vehicle in the windward direction; C_D is the wind resistance coefficient, which is a dimensionless quantity; A is the cross-sectional area of the vehicle (m^2); and ρ_a is the air density.

For the kinetic and potential energies, the derivatives at time t can be obtained as follows:

$$VSP = v[a(1 + \epsilon_i) + g(dg) + C_{Rg}] + 0.5\rho_a \frac{C_{pA}}{m} (v + v_w)^2 v \tag{12}$$

The calculation of the VSP can be represented by Eq 13:

$$VSP = 0.3227va + 0.0954v + 0.0000272v^3 \tag{13}$$

VSP is divided into different sections based on a given interval. Next, the average of all instantaneous emissions rates is calculated in each region as the emissions rate of this interval; this can effectively mitigate the discrete nature of the data and forecast vehicular emissions accurately using parameters based on the VSP.

Ref. [54] describes the relationship between VSP and the pollutant emissions rate, as shown in Table 1. This study uses VSP interval division and the corresponding pollutant emissions rate to calculate the traffic emissions of signalized intersections.

The vehicle emissions model based on the VSP distribution shown above can be expressed by Eq 14:

$$MOE_{e_j} = \sum_{i=1}^n f(p_i) \cdot R(p_{ij}) \tag{14}$$

where MOE_{e_j} is the j^{th} type of traffic emission along a route; i is the travel time ($i = 1, 2, 3, \dots, n$); p_i is the VSP value at time i ; $f(p_i)$ is the VSP distribution at time i when the VSP value is p_i ; and $R(p_{ij})$ is the j^{th} type of traffic emission rate when the VSP value is p_i at time i .

As a result, the vehicle emissions along the given route can be calculated based on the VSP distribution and the traffic emissions calculation model.

Different pollutants will produce different effects. This study uses the weighted average method to synthesize the different pollutants, and the influence of the unit is eliminated by normalized processing. Next, the expert scoring method is used to determine the weights of each indicator, whose values are 0.15, 0.7 and 0.15 [55]. Thus, the total traffic emissions described by Eq 15:

$$E = 0.15E_{VOC} + 0.70E_{CO} + 0.15E_{NO_x} \tag{15}$$

where E_{VOC} is the emission of volatile organic compounds (VOC); E_{CO} is the emission of carbon monoxide (CO); E_{NO_x} is the emission of nitrogen oxides (NO_x).

Relationship between delay and emissions

Considering a real traffic situation at an intersection, this study sets the free flow speed of the vehicles before entering the intersection to be $v_f = 70\text{km/h}$. The acceleration and deceleration functions of the vehicles are based on the method proposed in VISSIM when the speed is lower than 70 mph [48]:

$$a_d(t) = 2.74m/s^2 \tag{16}$$

$$a_a(t) = -0.04023v_a(t) + 3.5m/s^2 \tag{17}$$

This study quantifies the relationship between the control delay and the traffic emissions via regression analysis. The delay is changed from 0 to 40 seconds in steps of 0.1. When the speed

Table 1. VSP interval division and pollutant emissions rate.

VSP	NO _x (g/s)	VOC (g/s)	CO (g/s)
-20	0.00031	0.0033	0.02111
-19	0.00165	0.00276	0.01949
-18	0.00013	0.00248	0.02597
-17	0.00092	0.00215	0.02169
-16	0	0.00141	0.02173
-15	0.00015	0.0017	0.01875
-14	0.00068	0.00261	0.01864
-13	0.00042	0.00167	0.017
-12	0.00027	0.00119	0.01602
-11	0.00048	0.00158	0.02227
-10	0.00045	0.00129	0.0226
-9	0.00019	0.00149	0.0246
-8	0.00027	0.00218	0.02187
-7	0.00035	0.00157	0.02212
-6	0.00019	0.00196	0.02437
-5	0.00039	0.00152	0.02378
-4	0.00046	0.00168	0.03078
-3	0.00026	0.0022	0.029
-2	0.00027	0.00237	0.02226
-1	0.00043	0.00173	0.0255
0	0.00011	0.00082	0.00582
1	0.00053	0.00292	0.04613
2	0.00184	0.00463	0.06289
3	0.00302	0.00458	0.06795
4	0.00402	0.0046	0.07323
5	0.00421	0.00548	0.0816
6	0.00496	0.0059	0.08184
7	0.00586	0.00785	0.09112
8	0.00736	0.00663	0.09895
9	0.0083	0.00829	0.00829
10	0.00923	0.00824	0.11238
11	0.01178	0.00936	0.11265
12	0.0125	0.00921	0.14685
13	0.01402	0.01045	0.13741
14	0.01491	0.00917	0.15765
15	0.01643	0.01207	0.16011
16	0.01878	0.0126	0.16208
17	0.01924	0.01456	0.15508
18	0.02129	0.01438	0.14174
19	0.02199	0.01641	0.18483
20	0.02203	0.01501	0.16303

doi:10.1371/journal.pone.0146018.t001

decreases from $v_f = 70\text{km/h}$ to zero, the required time is calculated using Eq 18:

$$t = v_f/a_z(t) \tag{18}$$

Therefore, when the control delay is between 0 and 2 s, the vehicle will decelerate and then accelerate; it will not be idle. For example, when the control delay is 1.5 s, then the vehicle

decelerates with $a_d(t) = 2.74m/s^2$, and the speed at time 1.5 s can be calculated using:

$$v = v_f - a_d(t) \times t \tag{19}$$

The VSP value when a vehicle is decelerating or accelerating to $v_f = 70km/h$ can also be calculated as follows; this process requires an amount of time t:

$$\tau = \ln\left(v_a(t) / \left(\frac{b}{a}\right) + 1\right) / a \tag{20}$$

$$S_a(t) = \frac{b}{a^2} (e^{at} - at - 1) \tag{21}$$

Based on the vehicle trajectory, the emissions calculated based on VSP is 7.106785597 mg. Using the above Eqs 16-21, the threshold of vehicle delay is obtained as follows:

$$D_c = \left(t_d - \frac{S_d}{v_f}\right) + \left(t_a - \frac{S_a}{v_f}\right) = 2.0 \text{ s} \tag{22}$$

When the control delay is less than 2.0 seconds, the vehicle is not idle. When the control delay is more than 2 seconds, in addition to completing the movement processes of acceleration and deceleration, an idle process is also performed. As shown in Fig 2, emissions tend to increase with the control delay.

As a result, the relationship between the delay and the associated emissions is described by Eq 23:

$$y = 0.0538x^2 - 1.6877x + 106.07 \tag{23}$$

where y is the amount of emissions produced, and x is the value of the control delay.

The dissipation time during queuing while the green signal is illuminated is calculated as follows:

$$t_{B1} = ER \cdot q_d / (s - q_d) \tag{24}$$

where ER represents the effective green signal time, q_d represents the arrival flow rate and S represents the saturation flow rate.

The total time that a vehicle is blocked from movement at the intersection is the sum of the red signal time and the time that queuing dissipates during the green signal:

$$t_{B2} = ER + t_{B1} = ER \cdot S / (s - q_d) \tag{25}$$

As a result, the control delay of the vehicles is calculated as:

$$q_B = q_d \cdot \frac{t_{B2}}{CL} \tag{26}$$

where CL is the cycle time.

Thus, the emissions of one direction's traffic flow at the intersection under the control of the traffic signal control is obtained as follows:

$$Em_i(ER_i, CL) = \int_0^{ER_i} \left(\frac{1}{ER_i} \cdot y \cdot q_B\right) dx = \frac{1}{ER_i} \times \left(0.538 \times \frac{1}{3} \times ER_i^3 - 1.6877 \times \frac{1}{2} ER_i^2 + 106.07 \times ER_i\right) \times q_B \tag{27}$$

where $Em_i(ER_i, CL)$ represents the traffic emissions of the traffic flow i within one hour.

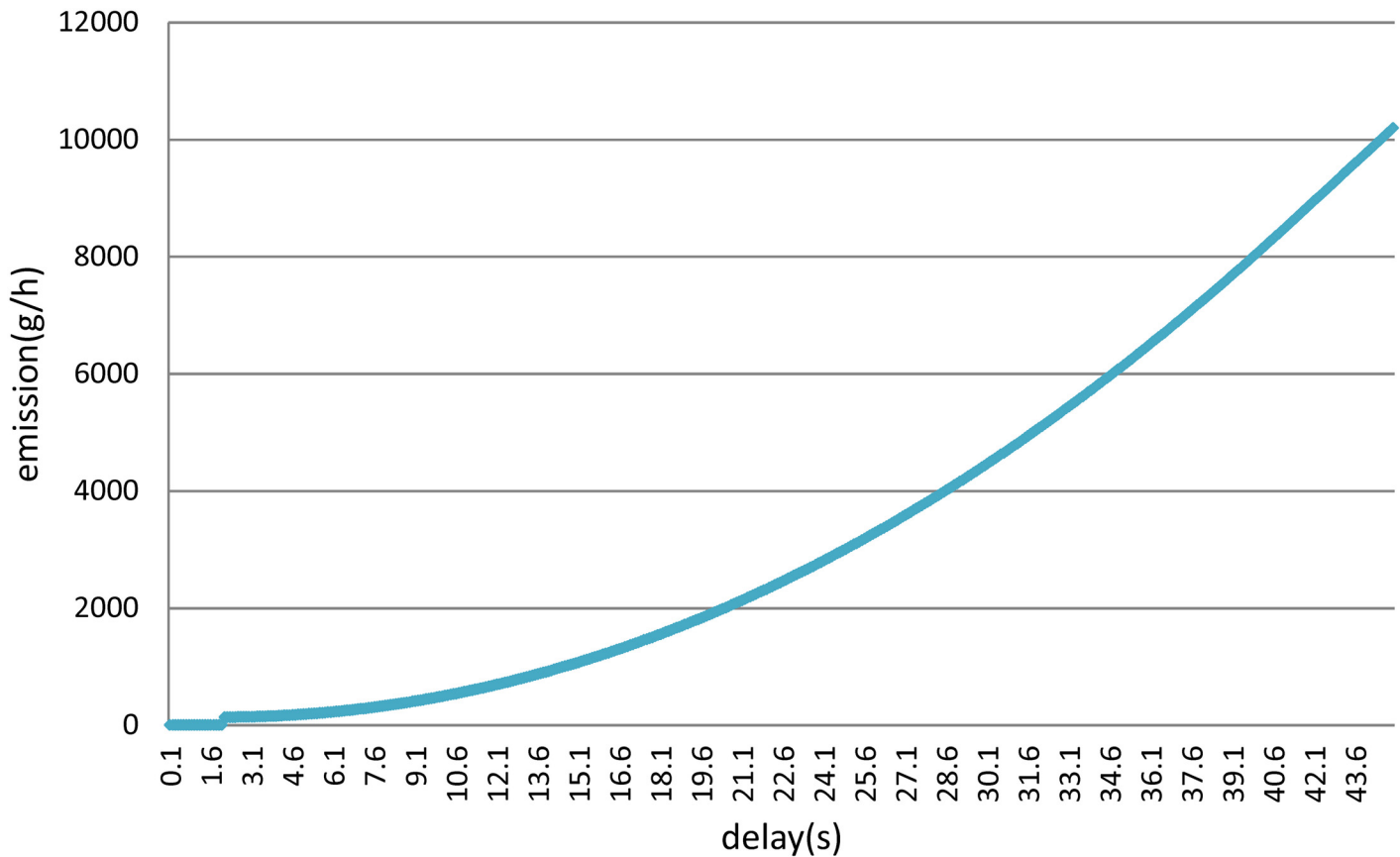


Fig 2. Relationship between delay and emissions.

doi:10.1371/journal.pone.0146018.g002

Delay calculation

This study uses the HCM2000 delay equation to calculate the intersection vehicle delay[38, 55]:

$$d = d_1 + d_2 \tag{28}$$

$$d_1 = \frac{0.5C(1 - \lambda)^2}{1 - [\min(1, X)\lambda]} \tag{29}$$

$$d_2 = 900T \left[(X - 1) + \sqrt{(X - 1)^2 + \frac{8kIX}{cT}} \right] \tag{30}$$

where d is the control delay (s); d_1 is the even delay (s); d_2 is the incremental delay (s); λ is the split; X is the saturation; C is the cycle time; c is the capacity (vehicles/h); T is the duration of the analysis (h); and k is the incremental delay correction factor of sensor control, where k is equal to 0.5 for a given signal cycle; and I is the incremental delay correction factor for vehicles to change lanes in the upstream channel, and the value of this factor is 1.0.

Using the above information, the total delay of the intersection can be obtained:

$$D = \sum_{j=1}^n (d_j \times q_j) \tag{31}$$

where d_j is the average vehicle control delay of j_{th} traffic signal phase of the intersection; q_j is the traffic flow of j_{th} traffic signal phase of the intersection.

Overall operating efficiency model for intersections

The key to a multi-objective optimization problem is determining how to combine and achieve various objectives. To achieve optimal control, we transform the multi-objective programming problem described above into a traditional single-objective programming problem using the utility optimization model. Different units of delay and emission are also considered, and the following model is established after normalization:

$$PI = \alpha \cdot \frac{D}{D_0} + \beta \cdot \frac{E}{E_0} \tag{32}$$

where PI is the comprehensive benefit function value; α is the weight of the delay; β is the weight of emissions; D and E are the total delay time and total amount of emissions of the intersection, respectively; and D_0 and E_0 are the initial values of the delay of the signal timing and the emissions, respectively.

The value of PI varies based on α and β . When α is equal to 1 and β is equal to 0, the operational benefit of a given intersection depends only on the length of the delay.

Solution algorithm

A proper cycle time can ensure that vehicles move through an intersection in an orderly and smooth manner. When traffic flow is slow, the cycle length should be small (i.e., generally no less than $15n$, where n is the phase number of the intersections) because a short period of time can cause vehicles to queue in the intersection, thus affecting traffic safety. When traffic flow is high, the capacity should be the highest priority, and the cycle time should be long but not more than 200 seconds, considering the psychology of driver boredom and the tendency of vehicle drivers to run red lights. As a result, the value of the cycle time should be defined as follows:

$$15n \leq C \leq 200s \tag{33}$$

When the saturation satisfies $0.8 \leq V/C \leq 1$, the operating conditions can be regarded as good, and the optimization function $PI(C)$ can be constrained as follows:

$$x_i = \frac{y_i}{\lambda_i} \tag{34}$$

$$0.8 \leq x_i \leq 1.0 \tag{35}$$

In this study, a comprehensive enumeration method is used to optimize the model. The specific optimization process used is shown in [Fig 3](#).

Step 1. Define the search range of cycle C as $15n-200s$, where n is the number of phases.

Step 2. Define the search interval of cycle C as $1s$.

Step 3. Set $C = 15n$ and $C_0 = 15n$.

Step 4. Calculate the value of $PI(C_0)$.

Step 5. Calculate the value of $PI(C)$.

Step 6. Calculate the saturation x_i . If $0.8 \leq x_i \leq 1.0$, then go to Step 7; otherwise, go to Step 9.

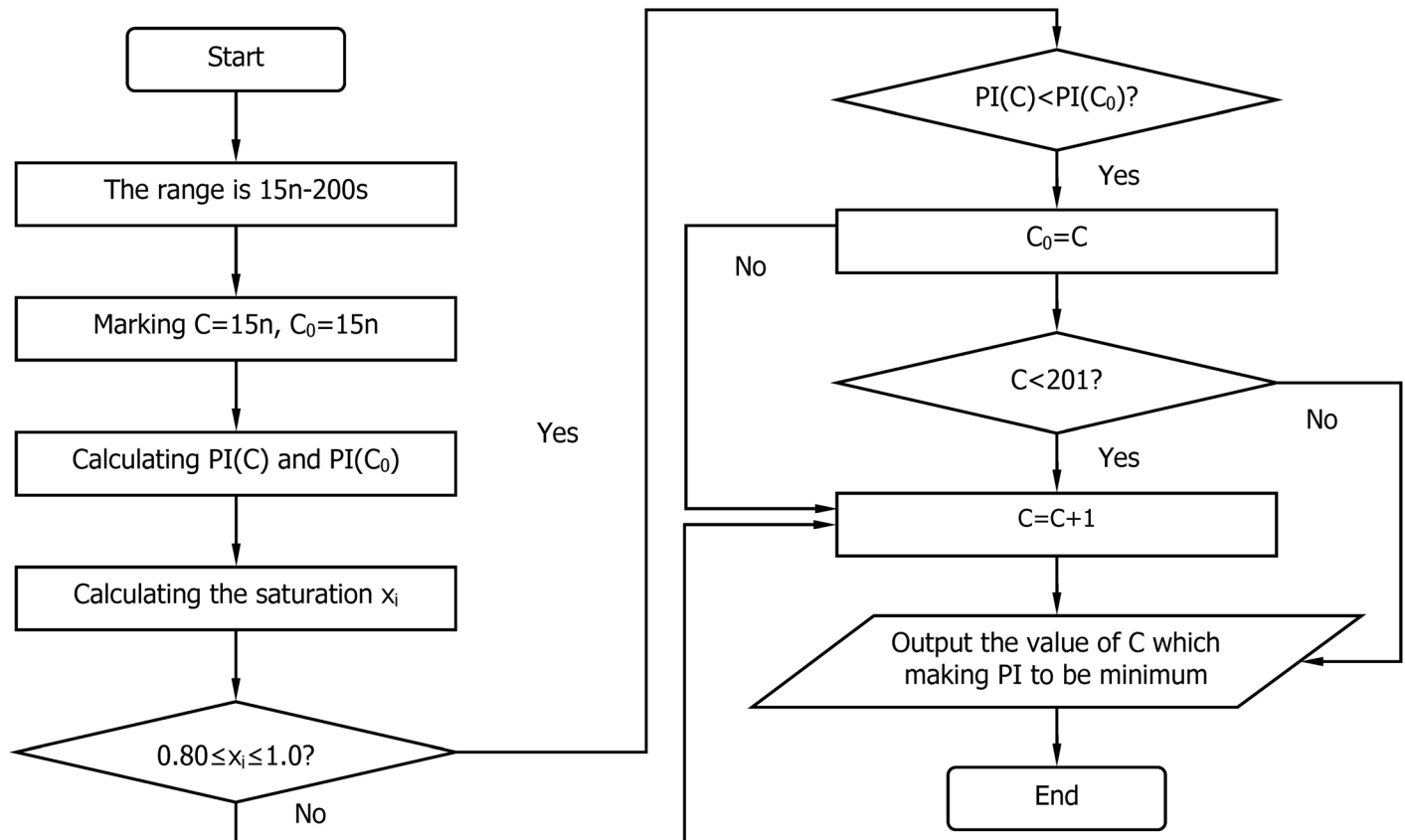


Fig 3. Cycle optimization flow chart.

doi:10.1371/journal.pone.0146018.g003

Step 7. If $PI(C) < PI(C_0)$, then $C_0 = C$.

Step 8. If $C < 201$, then go to Step 9; otherwise, end the process.

Step 9. Perform $C = C + 1$.

Step 10. Go Step 4.

After optimization, the cycle that meets the minimum value of PI can be obtained. Next, use the principle of equal saturation to determine the signal timing design for the intersection and choose the optimized timing instead of the original timing. As mentioned above, a smaller value of PI corresponds to better control of the emissions and delay; thus, we can effectively optimize the signal timing of a given intersection.

Results

Input data

To verify the method described above, this study considers the Renmin-Ziyou intersection in Changchun city. The geometric, signal control and traffic flow information of this intersection were collected from the field. The geometric features of the intersection are shown in Fig 4. Traffic flow data were obtained from loop-coil vehicle detectors and video camera vehicle detectors from August 10 to 23, 2014. The traffic flow data were provided and permitted to use by Changchun traffic police detachment of public security. The interval between data collection

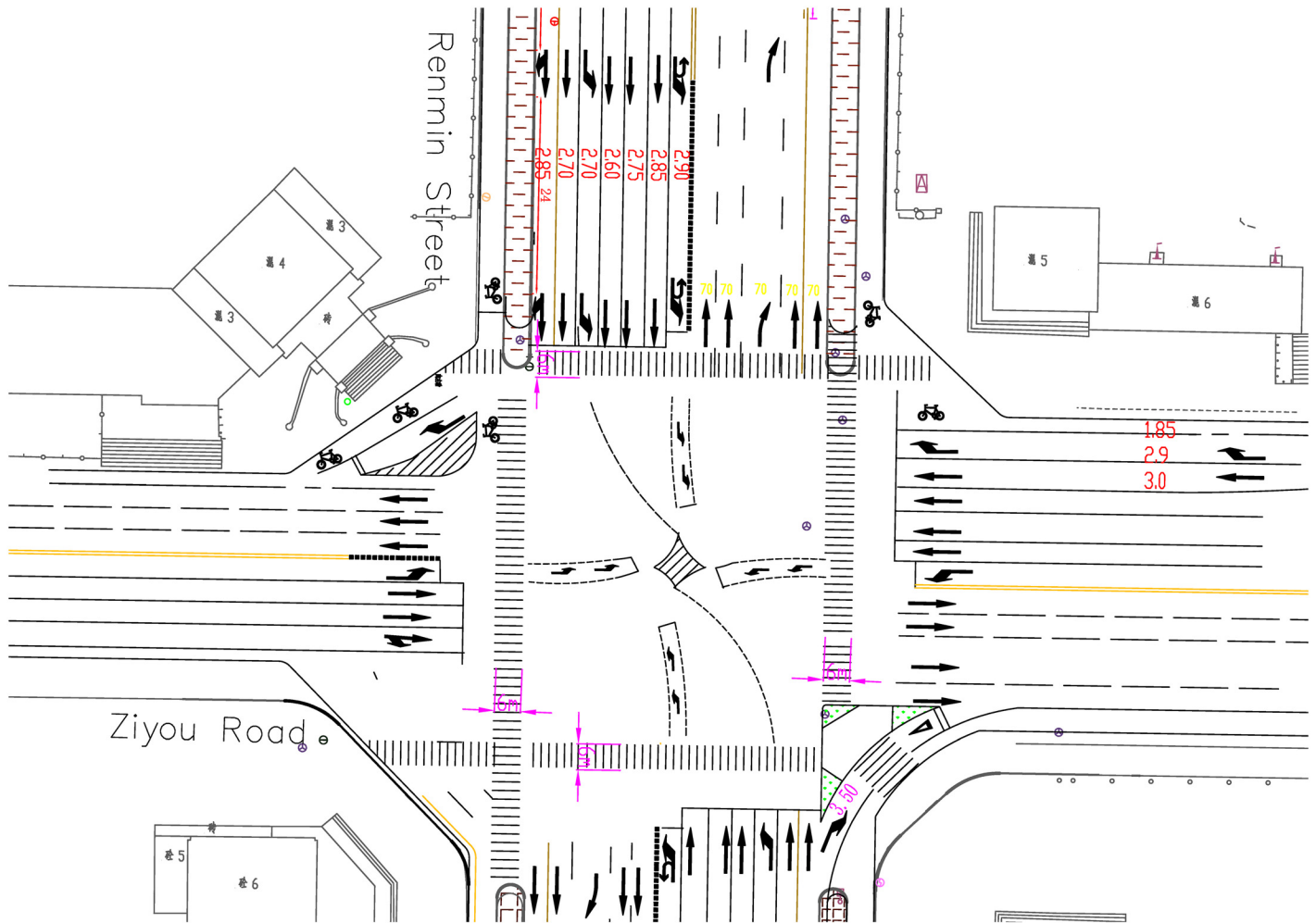


Fig 4. Geometric characteristics of the Renmin-Ziyou intersection in Changchun city.

doi:10.1371/journal.pone.0146018.g004

events was 5 minutes. These detectors collect various traffic parameters, including traffic volume, speed and occupancy rate. The traffic flow data and intersection features were input into the microscopic traffic simulation software (VISSIM) to evaluate the traffic signal control performances and the average vehicle emissions.

During the investigation process, the traffic was determined to be primarily composed of buses and cars on the road; these types of vehicles are represented by a cart and a car, respectively. The conversion coefficient of the cart is 2.0, and the conversion coefficient of the small car is 1.0[34, 39]. In this study, the average speed of the vehicles is assumed to be 40 km/h, and the length of the approach is assumed to be 100 m. Based on the above information, the traffic volume of each phase's key traffic flow is obtained. The straight flow from north to south is 327/h, the left-turn flow from north to south is 244/h, the straight flow from west to east is 374/h, and the left-turn flow from west to east is 411/h. After obtaining the basic information of the intersection, we applied the model proposed in this study to obtain the initial delay and emissions of the intersection: the initial total delay was determined to be 8.2859×10^5 seconds, and the initial emissions were determined to be 2.3969×10^4 grams per hour.

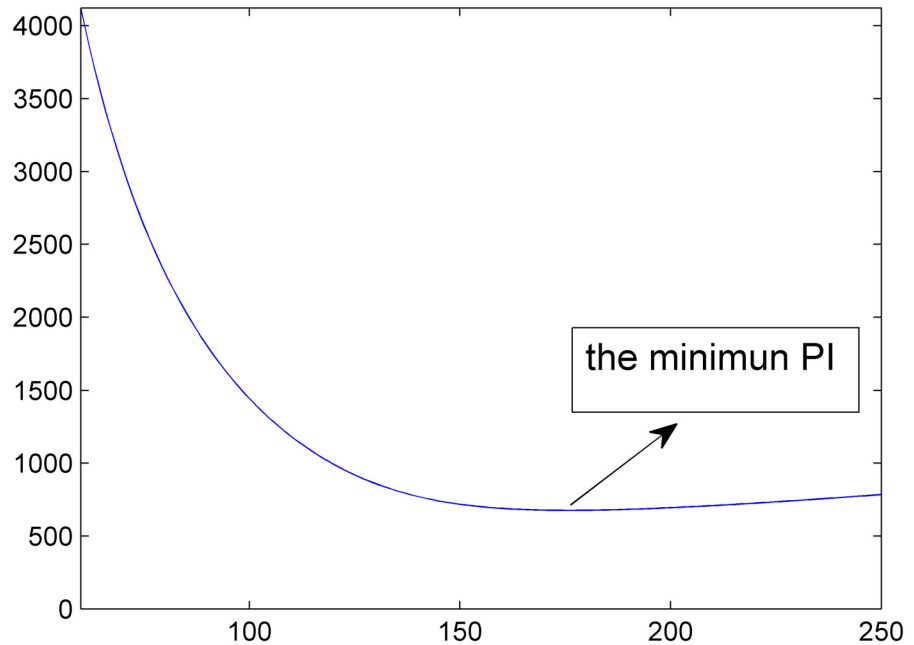


Fig 5. PI as the cycle changes.

doi:10.1371/journal.pone.0146018.g005

Simulation parameters

As mentioned above, the enumeration method is used to optimize the model and to limit it within the saturation and cycle. To improve the optimization efficiency, this study used MATLAB to solve the model. In the programming process of the enumeration methods, the calculation procedures for *PI* are used many times. As a result, this study modularizes this portion of the programming and uses the function $PI = zibianhanshu(C)$. Fig 5 shows the changes in *PI* as the cycle changes, and a cycle that achieves the minimum value of *PI* is identified, as expected. Next, this study determined this cycle by applying the method of enumeration.

Based on the optimization algorithm and real survey data, $C = 176$ yields the minimum *PI*. This optimization cycle is less than the original (216 s) and within the limits defined above, which allows the driver to accept the longer red light without too much impatience. Next, the equal saturation principle is used to calculate the optimal timing plan. The original timing plan and the optimized timing plan are shown in the Figs 6 and 7 as below.

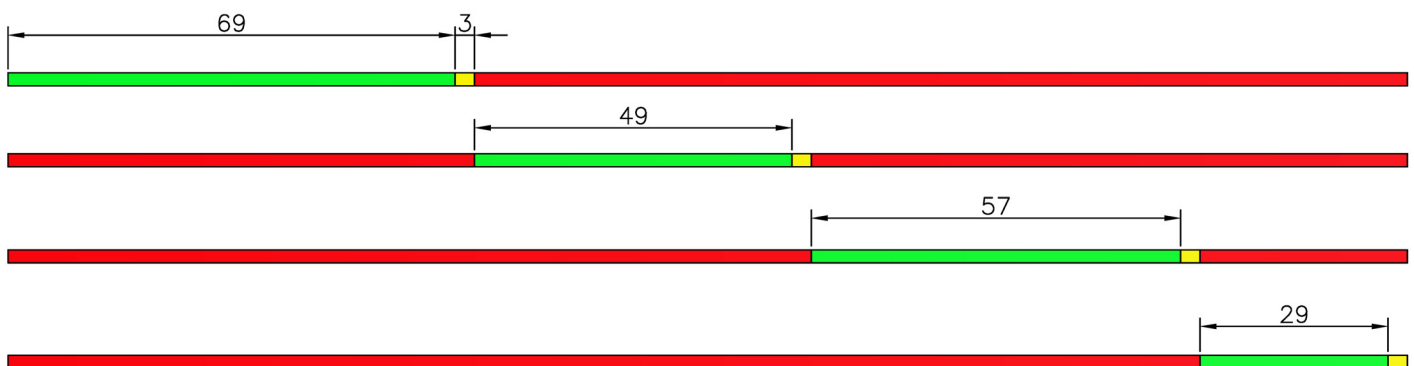


Fig 6. Original timing plan.

doi:10.1371/journal.pone.0146018.g006

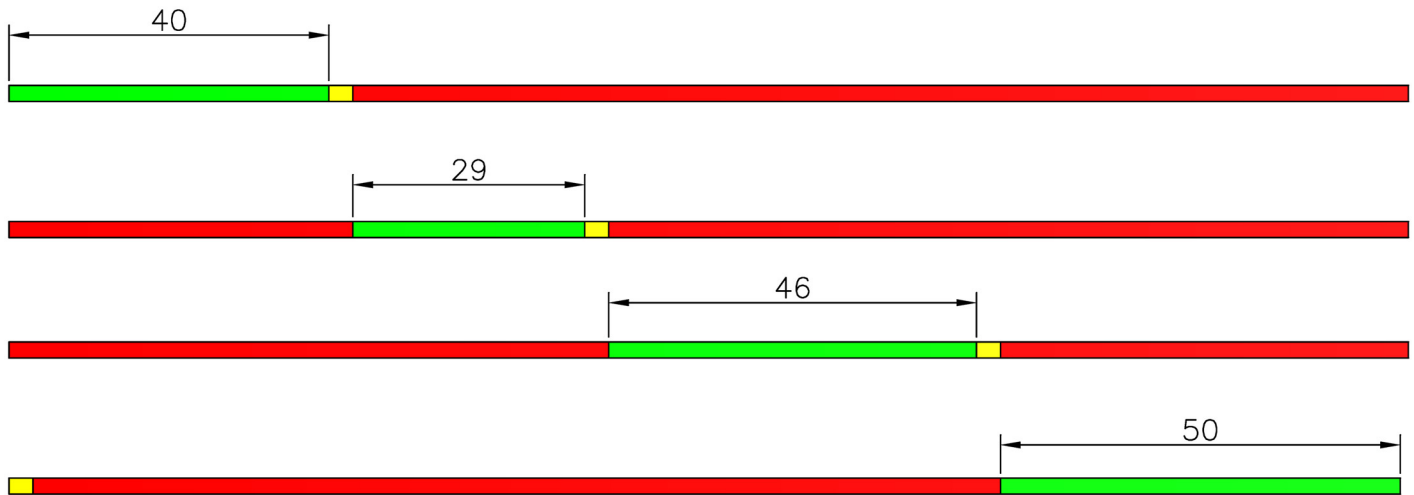


Fig 7. Optimized timing plan.

doi:10.1371/journal.pone.0146018.g007

Simulation implementation

Using VISSIM to simulate the intersection before and after changing the traffic signals, the effect of optimizing the delay and emissions is determined. The delay and emissions are compared based on the simulations before and after changing the signal control; these results are shown in Tables 2 and 3 and Fig 8.

From the data in the table, it is shown via comparison that both the delay and emissions are improved after optimization. The results show that changing the signal timing is effective; thus, using the model proposed in this study to optimize timing can improve the running status of an intersection and achieve the goal of this paper. The model considers the emissions and delay factors concurrently, improving the efficiency of the traffic and the environment.

Conclusions

Effective traffic signal control is required to ensure smooth and orderly operation of urban road traffic; such control is currently a popular research topic of many scholars. However, previous studies primarily focused on reducing traffic congestion and ignoring the influence of traffic on the environment. With the growing consciousness of people regarding environmental protection, a traffic signal control scheme that considers environmental effects is required; therefore, this article focused on the development of such a scheme. A multi-objective study of

Table 2. Contrast of the delay before and after optimization.

	Original plan	Optimized plan
delay (s)	56.62333333	55.76789474

doi:10.1371/journal.pone.0146018.t002

Table 3. Contrast of the emissions before and after optimization.

	VOC	NO _x	CO
Before	17.54935417	14.7330625	75.72191667
After	15.19551394	12.75681531	65.56557233

doi:10.1371/journal.pone.0146018.t003

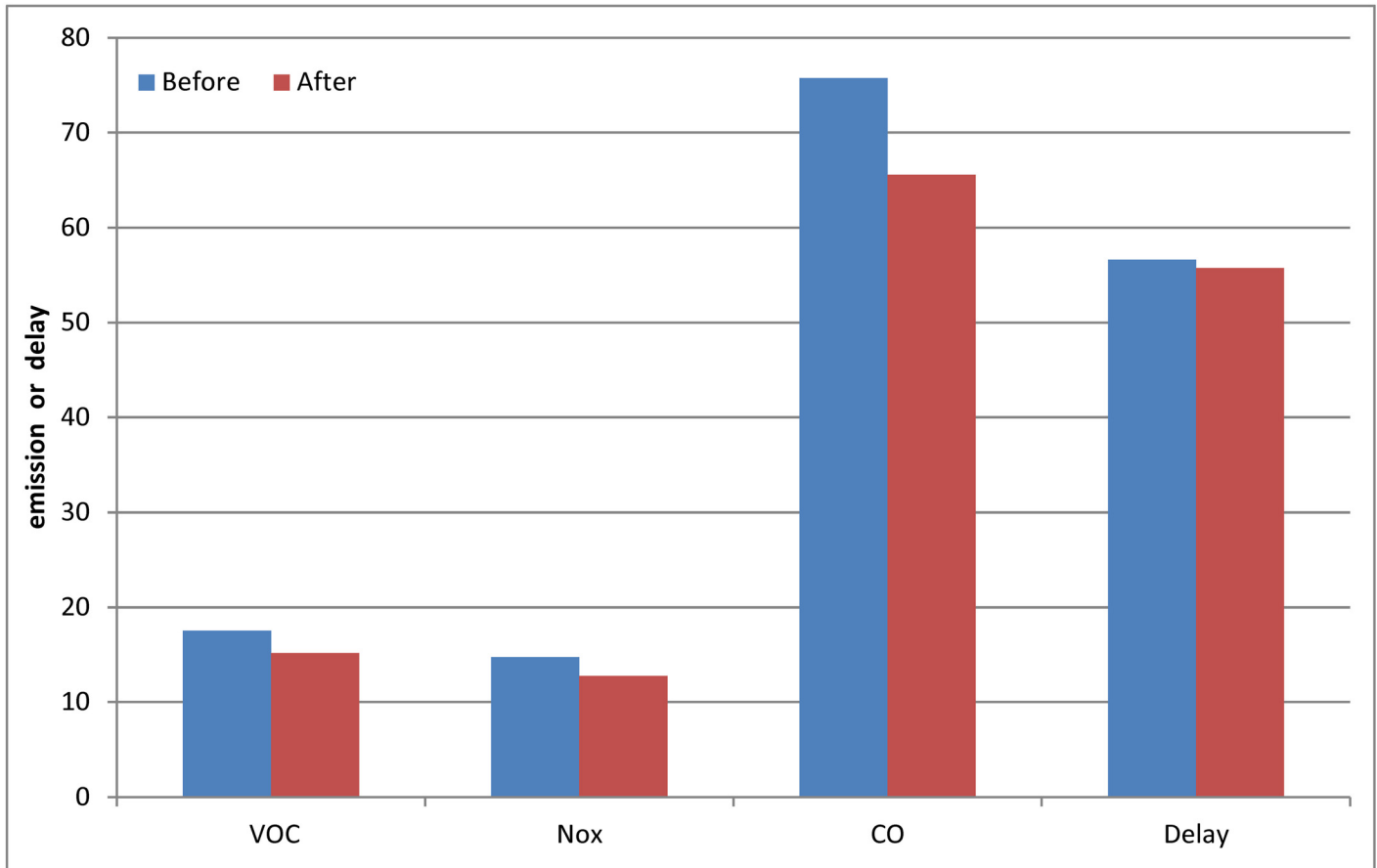


Fig 8. Contrast of related indices before and after optimization.

doi:10.1371/journal.pone.0146018.g008

traffic signal control was performed in view of the present development trend of traffic signal control; emissions were regarded as one of the goals for improving the operation of intersections to optimize the intersections based on vehicular delay.

Urban traffic signal control is a complex topic. The development described in this study addresses only one aspect of the topic (i.e., the primary stage) with results that are only applicable for a single intersection when considering both emissions and delay. Related research for arterial coordination and regional coordination was not considered in this article; such topics will be considered in a follow-up study and discussed in depth.

Acknowledgments

We thank ZS Yang and DX Yu for their help in traffic data collection and analysis. We also thank two anonymous reviewers for their constructive criticisms of an earlier version of this study.

Author Contributions

Conceived and designed the experiments: LCY GBW QX. Performed the experiments: LCY GBW QX. Analyzed the data: LCY GBW QX. Contributed reagents/materials/analysis tools: LCY GBW QX. Wrote the paper: LCY QX. Designed the software used in analysis: GBW.

References

1. Tang T-Q, Xu K-W, Yang S-C, Ding C. Impacts of SOC on car-following behavior and travel time in the heterogeneous traffic system. *Physica A: Statistical Mechanics and its Applications*. 2016; 441:221–9. doi: [10.1016/j.physa.2015.09.003](https://doi.org/10.1016/j.physa.2015.09.003)
2. Peng GH, Song W, Peng YJ, Wang SH. A novel macro model of traffic flow with the consideration of anticipation optimal velocity. *Physica A: Statistical Mechanics and its Applications*. 2014; 398:76–82. doi: [10.1016/j.physa.2013.12.015](https://doi.org/10.1016/j.physa.2013.12.015)
3. Zhu W-X, Zhang C-H. Analysis of energy dissipation in traffic flow with a variable slope. *Physica A: Statistical Mechanics and its Applications*. 2013; 392(16):3301–7. doi: [10.1016/j.physa.2013.04.004](https://doi.org/10.1016/j.physa.2013.04.004)
4. Tang T-Q, Yu Q. Influences of vehicles' fuel consumption and exhaust emissions on the trip cost without late arrival under car-following model. *Int J Mod Phys C*. 2016; 27(0):1650011. doi: [10.1142/S012918311650011X](https://doi.org/10.1142/S012918311650011X)
5. Yu SW, Shi ZK. Fuel consumptions and exhaust emissions induced by cooperative adaptive cruise control strategies. *Int J Mod Phys B*. 2015; 29(14). WOS:000355015500004.
6. Zhang N, Zhou P, Kung C-C. Total-factor carbon emission performance of the Chinese transportation industry: A bootstrapped non-radial Malmquist index analysis. *Renewable and Sustainable Energy Reviews*. 2015; 41:584–93. doi: [10.1016/j.rser.2014.08.076](https://doi.org/10.1016/j.rser.2014.08.076)
7. Tang TQ, Yu Q, Yang SC, Ding C. Impacts of the vehicle's fuel consumption and exhaust emissions on the trip cost allowing late arrival under car-following model. *Physica A: Statistical Mechanics and its Applications*. 2015; 431:52–62. doi: [10.1016/j.physa.2015.02.041](https://doi.org/10.1016/j.physa.2015.02.041) WOS:000354589200005.
8. Tang TQ, Li JG, Wang YP, Yu GZ. Vehicle's fuel consumption of car-following models. *Sci China Technol Sc*. 2013; 56(5):1307–12. doi: [10.1007/s11431-013-5182-9](https://doi.org/10.1007/s11431-013-5182-9) WOS:000318182000030.
9. Minocha VK, Saini G. Discussion of "Estimating vehicle fuel consumption and emissions based on instantaneous speed and acceleration levels" by Kyoung Ahn, Hesham Rakha, Antonio Trani, and Michel Van Aerde. *J Transp Eng-Asce*. 2003; 129(5):578–9. WOS:000184747200014.
10. Rakha H, Ahn K. Closure to "Estimating vehicle fuel consumption and emissions based on instantaneous speed and acceleration levels" by Kyoung Ahn, Hesham Rakha, Antonio Trani, and Michel Van Aerde. *J Transp Eng-Asce*. 2003; 129(5):579–81. WOS:000184747200015.
11. Ahn K, Rakha H, Trani A, Van Aerde M. Estimating vehicle fuel consumption and emissions based on instantaneous speed and acceleration levels. *J Transp Eng-Asce*. 2002; 128(2):182–90. WOS:000174040400010.
12. Ahn K. Microscopic fuel consumption and emission modeling [PhD Thesis]. Blacksburg: Virginia Polytechnic Institute and State University; 1998.
13. Tang T-Q, Huang H-J, Wu W-X, Wu Y-H. Analyzing trip cost with no late arrival under car-following model. *Measurement: Journal of the International Measurement Confederation*. 2015; 64:123–9. doi: [10.1016/j.measurement.2014.12.045](https://doi.org/10.1016/j.measurement.2014.12.045)
14. Tang T-Q, Li J-G, Yang S-C, Shang H-Y. Effects of on-ramp on the fuel consumption of the vehicles on the main road under car-following model. *Physica A: Statistical Mechanics and its Applications*. 2015; 419:293–300. doi: [10.1016/j.physa.2014.10.051](https://doi.org/10.1016/j.physa.2014.10.051)
15. Tang T-Q, Chen L, Wu Y-H, Caccetta L. A macro traffic flow model accounting for real-time traffic state. *Physica A: Statistical Mechanics and its Applications*. 2015; 437:55–67. doi: [10.1016/j.physa.2015.05.054](https://doi.org/10.1016/j.physa.2015.05.054)
16. Tang T-Q, Caccetta L, Wu Y-H, Huang H-J, Yang X-B. A macro model for traffic flow on road networks with varying road conditions. *Journal of Advanced Transportation*. 2014; 48(4):304–17. doi: [10.1002/atr.215](https://doi.org/10.1002/atr.215)
17. Yu SW, Shi ZK. An extended car-following model considering vehicular gap fluctuation. *Measurement*. 2015; 70:137–47. WOS:000354402000015.
18. Yu S, Shi Z. Dynamics of connected cruise control systems considering velocity changes with memory feedback. *Measurement: Journal of the International Measurement Confederation*. 2015; 64:34–48. doi: [10.1016/j.measurement.2014.12.036](https://doi.org/10.1016/j.measurement.2014.12.036)
19. Yu SW, Shi ZK. The effects of vehicular gap changes with memory on traffic flow in cooperative adaptive cruise control strategy. *Physica A*. 2015; 428:206–23. doi: [10.1016/j.physa.2015.01.064](https://doi.org/10.1016/j.physa.2015.01.064) WOS:000352328100020.
20. Tang TQ, Chen L, Yang SC, Shang HY. An extended car-following model with consideration of the electric vehicle's driving range. *Physica A*. 2015; 430:148–55. doi: [10.1016/j.physa.2015.01.014](https://doi.org/10.1016/j.physa.2015.01.014) WOS:000353854200016.

21. Tang TQ, Li JG, Huang HJ, Yang XB. A car-following model with real-time road conditions and numerical tests. *Measurement*. 2014; 48:63–76. doi: [10.1016/j.measurement.2013.10.035](https://doi.org/10.1016/j.measurement.2013.10.035) WOS:000329207400008.
22. Tang TQ, Shi WF, Shang HY, Wang YP. An extended car-following model with consideration of the reliability of inter-vehicle communication. *Measurement*. 2014; 58:286–93. doi: [10.1016/j.measurement.2014.08.051](https://doi.org/10.1016/j.measurement.2014.08.051) WOS:000344485600033.
23. Wu CX, Zhao GZ, Ou B. A fuel economy optimization system with applications in vehicles with human drivers and autonomous vehicles. *Transport Res D-Tr E*. 2011; 16(7):515–24. WOS:000294398200006.
24. Rakha HA, Ahn K, Moran K, Saerens B, Van den Bulck E. Virginia Tech Comprehensive Power-Based Fuel Consumption Model: Model development and testing. *Transport Res D-Tr E*. 2011; 16(7):492–503. WOS:000294398200003.
25. Wei S, Yu X. Study on stability and energy consumption in typical car-following models. *Physica A*. 2007; 381:399–406. doi: [10.1016/j.physa.2007.02.106](https://doi.org/10.1016/j.physa.2007.02.106) WOS:000247700900034.
26. Edwardes W, Rakha H. Virginia Tech Comprehensive Power-Based Fuel Consumption Model Modeling Diesel and Hybrid Buses. *Transportation Research Record*. 2014;(2428):1–9. WOS:000342877200001.
27. Rakha H, Van Aerde M, Ahn K, Trani AA. Requirements for evaluating traffic signal control impacts on energy and emissions based on instantaneous speed and acceleration measurements. *Transportation Research Record*. 2000;(1738):56–67. doi: [10.3141/1738-07](https://doi.org/10.3141/1738-07)
28. Osorio C, Nanduri K. Energy-Efficient Urban Traffic Management: A Microscopic Simulation-Based Approach. *Transport Sci*. 2015; 49(3):637–51. WOS:000359425900014.
29. Zhang LH, Yin YF, Chen SG. Robust signal timing optimization with environmental concerns. *Transport Res C-Emer*. 2013; 29:55–71. WOS:000317162000004.
30. Pandian S, Gokhale S, Ghoshal AK. Evaluating effects of traffic and vehicle characteristics on vehicular emissions near traffic intersections (vol 14, pg 180, 2009). *Transport Res D-Tr E*. 2013; 23:114-. WOS:000322297100016.
31. Pandian S, Gokhale S, Ghoshal AK. Evaluating effects of traffic and vehicle characteristics on vehicular emissions near traffic intersections. *Transport Res D-Tr E*. 2009; 14(3):180–96. WOS:000264699800004.
32. Ghafghazi G, Hatzopoulou M. Simulating the environmental effects of isolated and area-wide traffic calming schemes using traffic simulation and microscopic emission modeling. *Transportation*. 2014; 41(3):633–49. doi: [10.1007/s11116-014-9513-x](https://doi.org/10.1007/s11116-014-9513-x) WOS:000335245600011.
33. Redhu P, Gupta AK. Delayed-feedback control in a Lattice hydrodynamic model. *Commun Nonlinear Sci*. 2015; 27(1–3):263–70. doi: [10.1016/j.cnsns.2015.03.015](https://doi.org/10.1016/j.cnsns.2015.03.015) WOS:000353774500022.
34. El-Tantawy S, Abdulhai B, Abdelgawad H. Design of reinforcement learning parameters for seamless application of adaptive traffic signal control. *Journal of Intelligent Transportation Systems: Technology, Planning, and Operations*. 2014; 18(3):227–45. doi: [10.1080/15472450.2013.810991](https://doi.org/10.1080/15472450.2013.810991)
35. Ma XL, Jin JC, Lei W. Multi-criteria analysis of optimal signal plans using microscopic traffic models. *Transport Res D-Tr E*. 2014; 32:1–14. doi: [10.1016/j.trd.2014.06.013](https://doi.org/10.1016/j.trd.2014.06.013) WOS:000344212600001.
36. Gupta AK, Dhiman I. Analyses of a continuum traffic flow model for a nonlane-based system. *Int J Mod Phys C*. 2014; 25(10). WOS:000342160700002.
37. Gupta AK. A Section Approach to a Traffic Flow Model on Networks. *Int J Mod Phys C*. 2013; 24(5). WOS:000318526000001.
38. Lee CY, Jeffery R, Hutchinson G, Alison MR, Poulosom R, Wright NA, et al. Bone Marrow Cells in Murine Colitis: Multi-Signal Analysis Confirms Pericycatal Myofibroblast Engraftment without Epithelial Involvement. *Plos One*. 2011; 6(10). ARTN e26082 doi: [10.1371/journal.pone.0026082](https://doi.org/10.1371/journal.pone.0026082) WOS:000295978600039.
39. Srinivasan D, Choy MC, Cheu RL. Neural networks for real-time traffic signal control. *IEEE T Intell Transp*. 2006; 7(3):261–72. doi: [10.1109/tits.2006.874716](https://doi.org/10.1109/tits.2006.874716)
40. Li XG, Li GQ, Pang SS, Yang XG, Tian JL. Signal timing of intersections using integrated optimization of traffic quality, emissions and fuel consumption: a note. *Transport Res D-Tr E*. 2004; 9(5):401–7. doi: [10.1016/j.trd.2004.05.001](https://doi.org/10.1016/j.trd.2004.05.001) WOS:000224449400005.
41. Dickinson MW, Thornton AC, Graves S. Technology portfolio management: Optimizing interdependent projects over multiple time periods. *IEEE T Eng Manage*. 2001; 48(4):518–27. doi: [10.1109/17.969428](https://doi.org/10.1109/17.969428) WOS:000172642500009.
42. Niittymaki J, Nevala R. Fuzzy adaptive traffic signal control—Principles and results. Annual Conference of the North American Fuzzy Information Processing Society—NAFIPS. 2001; 5:2870–5. doi: [10.1109/nafips.2001.943682](https://doi.org/10.1109/nafips.2001.943682)

43. Ahn K, Rakha H, Trani A, Van Aerde M. Estimating vehicle fuel consumption and emissions based on instantaneous speed and acceleration levels. *Journal of Transportation Engineering*. 2002; 128(2):182–90. doi: [10.1061/\(asce\)0733-947x\(2002\)128:2\(182\)](https://doi.org/10.1061/(asce)0733-947x(2002)128:2(182))
44. Guo H, Zhang Q-y, Shi Y, Wang D-h. Evaluation of the International Vehicle Emission (IVE) model with on-road remote sensing measurements. *Journal of Environmental Sciences*. 2007; 19(7):818–26. doi: [10.1016/S1001-0742\(07\)60137-5](https://doi.org/10.1016/S1001-0742(07)60137-5)
45. Xiao Y, Zhao Q, Kaku I, Xu Y. Development of a fuel consumption optimization model for the capacitated vehicle routing problem. *Computers & Operations Research*. 2012; 39(7):1419–31. doi: [10.1016/j.cor.2011.08.013](https://doi.org/10.1016/j.cor.2011.08.013)
46. Samra S, El-Mahdy A, Wada Y. A Linear Time and Space Algorithm for Optimal Traffic-Signal Duration at an Intersection. *Ieee T Intell Transp*. 2015; 16(1):387–95. doi: [10.1109/Tits.2014.2336657](https://doi.org/10.1109/Tits.2014.2336657) WOS:000349391200033.
47. Gupta AK, Dhiman I. Phase diagram of a continuum traffic flow model with a static bottleneck. *Nonlinear Dynam*. 2015; 79(1):663–71. WOS:000348314500054.
48. Cesme B, Furth PG. Self-organizing traffic signals using secondary extension and dynamic coordination. *Transport Res C-Emer*. 2014; 48:1–15. doi: [10.1016/j.trc.2014.08.006](https://doi.org/10.1016/j.trc.2014.08.006) WOS:000345725600001.
49. Meszaros F, Torok A. Theoretical investigation of emission and delay based intersection controlling and synchronizing in Budapest. *Periodica Polytechnica Transportation Engineering*. 2014; 42(1):37–42. doi: [10.3311/PPtr.7183](https://doi.org/10.3311/PPtr.7183)
50. Wu YZ, Song GH, Yu L. Sensitive analysis of emission rates in MOVES for developing site-specific emission database. *Transport Res D-Tr E*. 2014; 32:193–206. doi: [10.1016/j.trd.2014.07.009](https://doi.org/10.1016/j.trd.2014.07.009) WOS:000344212600017.
51. Wang J, Xiong Z, Yan X. Fertilizer-induced emission factors and background emissions of N₂O from vegetable fields in China. *Atmospheric Environment*. 2011; 45(38):6923–9. doi: [10.1016/j.atmosenv.2011.09.045](https://doi.org/10.1016/j.atmosenv.2011.09.045)
52. Zhou P, Ang BW, Han JY. Total factor carbon emission performance: A Malmquist index analysis. *Energy Economics*. 2010; 32(1):194–201. doi: [10.1016/j.eneco.2009.10.003](https://doi.org/10.1016/j.eneco.2009.10.003)
53. Morrison GM, Yeh S, Eggert AR, Yang C, Nelson JH, Greenblatt JB, et al. Comparison of low-carbon pathways for California. *Climatic Change*. 2015. doi: [10.1007/s10584-015-1403-5](https://doi.org/10.1007/s10584-015-1403-5)
54. Xunan T. Signal Timing Optimization of Urban Street Intersection Based on Reducing Vehicle Pollutant Emissions. Beijing: Beijing Jiaotong University; 2014.
55. Board TR. Highway Capacity Manual. Washington DC.: TRB, 2000 Special Report 209.